

# Adsorption of dyes and phenol from water on resin adsorbents: Effect of adsorbate size and pore size distribution

Xiao Zhang<sup>a,b</sup>, Aimin Li<sup>a,c,\*</sup>, Zhenmao Jiang<sup>a</sup>, Quanxing Zhang<sup>a,c</sup>

<sup>a</sup> School of the Environment, and State Key Laboratory of Pollution Control and Resources Reuse, Nanjing University, Nanjing 210093, PR China

<sup>b</sup> Department of Environmental Sciences, Jiangsu Broadcasting and Television University, Nanjing 210038, PR China

<sup>c</sup> Research Center for Engineering Technology of Organic Pollutant Control and Resources Reuse of Jiangsu Province, Nanjing 210046, PR China

Received 27 December 2005; received in revised form 23 March 2006; accepted 23 March 2006

Available online 18 April 2006

## Abstract

Batch adsorption runs of two commercial reactive dyes (methylene blue and reactive orange X-GN) and phenol from water onto two resin adsorbents (Amberlite XAD-4, a macroreticular adsorbent and ZCH-101, a hyper-cross-linked adsorbent) were carried out in the present study. Effect of adsorbate size and pore structure of the resin adsorbents on adsorption was discussed and Langmuir and Freundlich models were tested for the relevant adsorption isotherms. In the kinetic section concentration–time profiles were obtained to further elucidate the effect of adsorbate size and porous structure on adsorption mechanism. A pseudo-second-order model was proved to give a satisfactory description of the related kinetic results. Two-stage kinetic curve of methylene blue onto ZCH-101 was observed at a specific experimental condition and modeled schematically according to its specific pore size distribution. Furthermore, other kinetic experiments were performed at different ambient temperature to validate the proposed schematic model.

© 2006 Elsevier B.V. All rights reserved.

**Keywords:** Adsorption; Resin adsorbent; Adsorbate size; Pore size distribution; Kinetics

## 1. Introduction

Liquid-phase adsorption has been shown to be highly efficient for removal of dyes and phenol from process or waste effluents [1–7]. As regards the adsorbents, granular or powdered activated carbons are widely used because of their excellent adsorption capability for the target pollutants [6]. However, their use is limited in field application by their high cost and poor mechanical strength. In the past two decades synthetic resin adsorbents have often been regarded as an alternative of activated carbon since they can be easily regenerated and chemical pollutants can be recovered after regeneration of the adsorbents [2–5,8]. In some industrial fields, synthetic resin adsorbents were also used and designed as specific adsorption applications [9,10]. Comparatively, though adsorption of organic pollutants onto resin adsorbents has achieved considerable attention, the related adsorption mechanism is still not well understood and needs

further study. Specially, the importance of porous structure on adsorption of many contaminants in aqueous solution is not well understood. As to physisorption on porous materials, it's generally accepted that adsorption mechanism and process may be significantly different as a consequence of porous structure. In the IUPAC classification of pore size [11], the definitions of 'macropores', 'mesopores' and 'micropores' depend on the different adsorption mechanism at pores with specified range of width: in micropores the whole accessible volume is regarded as adsorption space and the process occurs due to micropore filling [12], as distinct from surface coverage which takes place on the walls of macropores. On the other hand, physisorption in mesopores takes place in two more or less stages (monolayer–multilayer adsorption and capillary condensation). For instance, Sing [13] concluded that mesopores are thought to be important in air/soil adsorption system for the diffusion of air and the transport and distribution of water, while the wider macropores provide channels for easy removal of surplus water and allow air to penetrate rapidly to the required depth. In liquid/solid system, although the pore blockage effect [14] and displacement effect [15] of NOMs on atrazine adsorption by PACs were discussed before,

\* Corresponding author. Tel.: +86 25 83593104; fax: +86 25 83707304.  
E-mail address: [environzhang@e165.com](mailto:environzhang@e165.com) (A. Li).

there are still few references focusing on the effect of the pore structure and adsorbate size on adsorption.

In the present study we address the role of adsorbate size and pore structure of resin adsorbents in adsorption from aqueous solution. Methylene blue (MB), reactive orange X-GN (RO) and phenol were selected as adsorbate due to their different molecular size and ubiquity in water body. Two synthetic resin adsorbents (XAD-4, a macroporous polystyrene adsorbent and ZCH-101, a hyper-cross-linked polystyrene adsorbent) were chosen as adsorbent. To achieve the goal, batch isotherm and kinetic experiments were performed and modeled by different isotherm equations and the pseudo-second-order kinetic equation.

## 2. Experimental

### 2.1. Materials

#### 2.1.1. Adsorbents

The hyper-cross-linked resin adsorbent ZCH-101 was synthesized as follows: about 40 g of the chloromethylated styrene–divinylbenzene copolymer beads (provided kindly by Jinxiang Chemical, PR China. Its cross-linking density is about 8% and the chloral content is about 17%) was dried under vacuum at 328 K for 10 h and then swollen in 150 ml of nitrobenzene for 12 h. Two grams of zinc chloride was added gradually in the above system at 353 K under mechanical stirring. The mixture was further stirred at 383 K for 5 h and then cooled to 298 K to obtain the hyper-cross-linked resin adsorbent ZCH-101. Another resin adsorbent Amberlite XAD-4 was purchased from Rohm Hass Co., USA. Both adsorbents were extracted with ethanol for 8 h and then dried under vacuum at 323 K for 10 h and finally selected by 40–60 mesh sieves prior to use.

#### 2.1.2. Adsorbates

Methylene blue (MB), reactive orange X-GN (RO) and phenol used in this study are of analytical grade and were purchased

from Shanghai reagent station, China. Their concentrations in aqueous solution were determined by an UV–vis spectrometer (Heλ10SβUnicam, British) at 665, 476 and 270 nm, respectively. Also, their salient properties including the Newtonian ball and spring models are presented in Table 1 and Fig. 1.

### 2.2. Isotherm experiment

First 0.200 g resin samples were added to several 250 ml sealed flasks, a 100 ml aqueous solution containing known concentration of each adsorbate was then added into each flask. Afterwards the flasks were shaken at 200 rpm and a preset temperature in a G 25 model incubator shaker with thermostat (New Brunswick Scientific Co. Inc., UK) for 24 h to attain equilibrium. The amounts adsorbed by resin particles were calculated by the mass balance relation as given below:

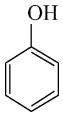
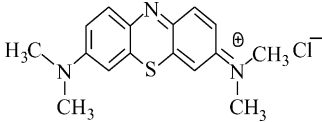
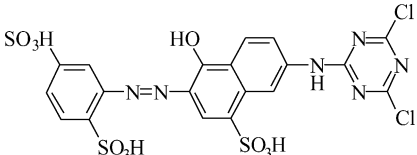
$$q_e = \frac{(C_0 - C_e) \times V}{W} \quad (1)$$

where  $C_0$  and  $C_e$  are the initial solution concentration and equilibrium concentration,  $V$  is the volume of solution and  $W$  is the weight of dry resin.

### 2.3. Kinetic studies

A series of 500 ml Erlenmeyer flasks containing a definite volume of MB, RO and phenol solution of known concentrations were kept in a thermostatic shaking water bath. After attaining the desired temperature, a known amount of the adsorbent was added to each flask and the flasks were allowed to agitate mechanically at an identical stirring speed of 120 rpm [16]. In the previous study, negligible effect of the stirring speed was observed on mass transfer of the solutes used in the paper from bulk solution to the surface of ZCH-101 and XAD-4 when the stirring speed was controlled at larger than 120 rpm. At given time intervals, about 0.1 ml of solution was sampled and analyzed for MB, RO and phenol as mentioned above. All of the

Table 1  
Properties of phenol and two dyes

Substance	Formula	Structure	Molecular weight	Molecular size <sup>a</sup>
Phenol	C <sub>6</sub> H <sub>6</sub> O		94.1	0.57 nm × 0.42 nm × 0.02 nm
MB	C <sub>16</sub> H <sub>18</sub> N <sub>3</sub> SCl		319.8	1.42 nm × 0.62 nm × 0.16 nm
RO	C <sub>19</sub> H <sub>12</sub> Cl <sub>2</sub> N <sub>6</sub> O <sub>10</sub> S <sub>3</sub>		651.4	1.97 nm × 0.80 nm × 0.23 nm

<sup>a</sup> Determined by software Chemoffice.

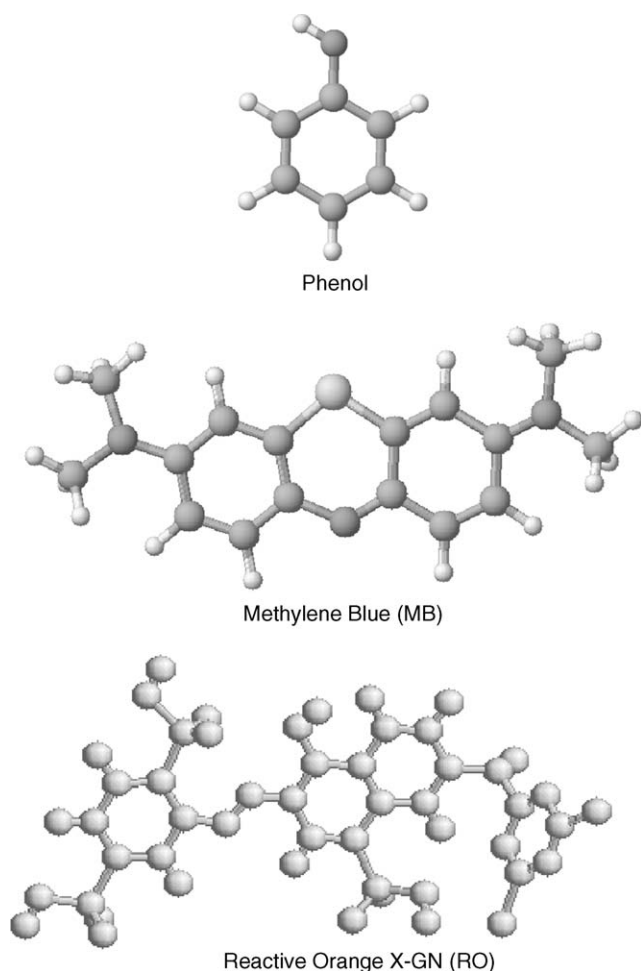


Fig. 1. Newtonian ball and spring models of phenol, MB and RO.

experiments were carried out three times at the identical conditions to ensure its recurrence.

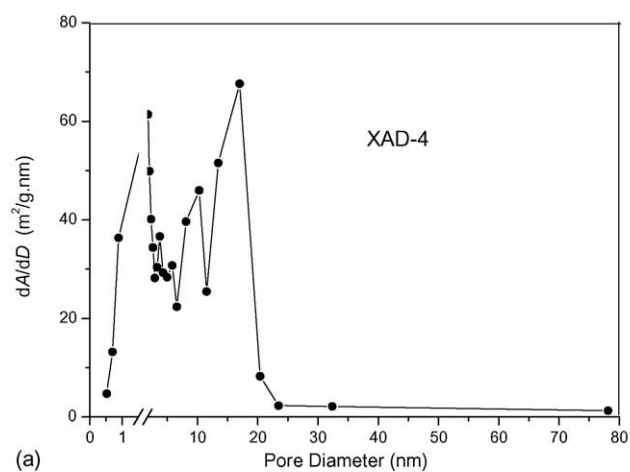
### 3. Results and discussion

#### 3.1. Characterization of resin adsorbents

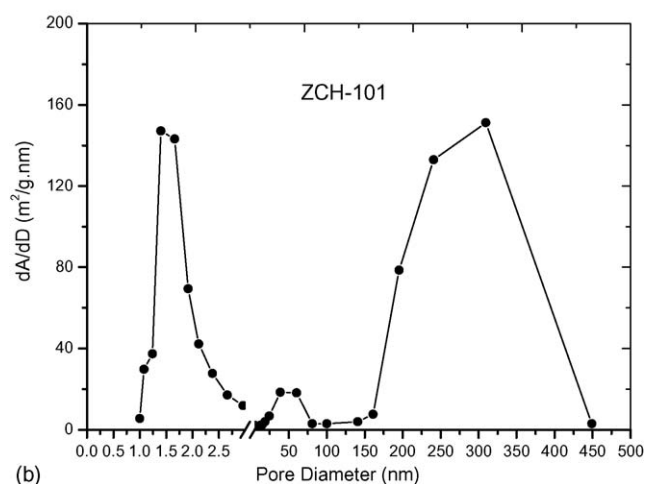
Both resin adsorbents employed in the study were analyzed by ASAP 2010 (Micrometrics, Australia) and the detailed properties are shown in Table 2 and Fig. 2. It should be noticeably

Table 2  
Salient properties of resin adsorbents

Property	ZCH-101	Amberlite XAD-4
Matrix	Styrene–divinylbenzene	Styrene–divinylbenzene
BET surface area (m <sup>2</sup> /g)	804.0	868.4
Micropore area (m <sup>2</sup> /g)	481.5	54.0
Mesopore area (m <sup>2</sup> /g)	79.3	391.5
Micropore volume (cm <sup>3</sup> /g)	0.22	0.0043
Total pore volume (cm <sup>3</sup> /g)	0.58	1.22
Average pore width (nm)	2.89	5.61
Particle size (mm)	0.22–0.45	0.22–0.45



(a)



(b)

Fig. 2. Pore size distribution of resin adsorbents XAD-4 and ZCH-101.

that ZCH-101, a hyper-cross-linked resin adsorbent, presents a bimodal pore size distribution at 1.0–2.5 nm and at larger than 150 nm in diameter. This is in agreement with the results reported by Oh et al. [17] and Tayurupa et al. [18]. But most of the pore region of another adsorbent, XAD-4, is displayed in a continuous range of 0.5–20 nm in diameter. Another observation is, though BET surface area of both adsorbents approaches to each other, the microporous area of ZCH-101 is about 10-fold greater than XAD-4 while their mesoporous area is ordered reversely. Due to different adsorption mechanism on micropore and mesopore region of solid adsorbent [19], effect of pore structure on adsorption should be noteworthy.

#### 3.2. Adsorption isotherm

Adsorption isotherms of three adsorbates on both resin adsorbents are depicted in Fig. 3(a–c). As shown in Fig. 3(a), adsorption capacity of phenol, the smallest adsorbate in molecular size in the present study, on ZCH-101 is much larger than on XAD-4, which may attribute to the larger micropore region of ZCH-101 [20]. For MB adsorption concerned, the amount loaded on XAD-4 is, on the contrary, larger than ZCH-101. Due to its larger size in molecular diameter, it is believable that part of the micropore structure of resin adsorbent (less than the molecular size of MB

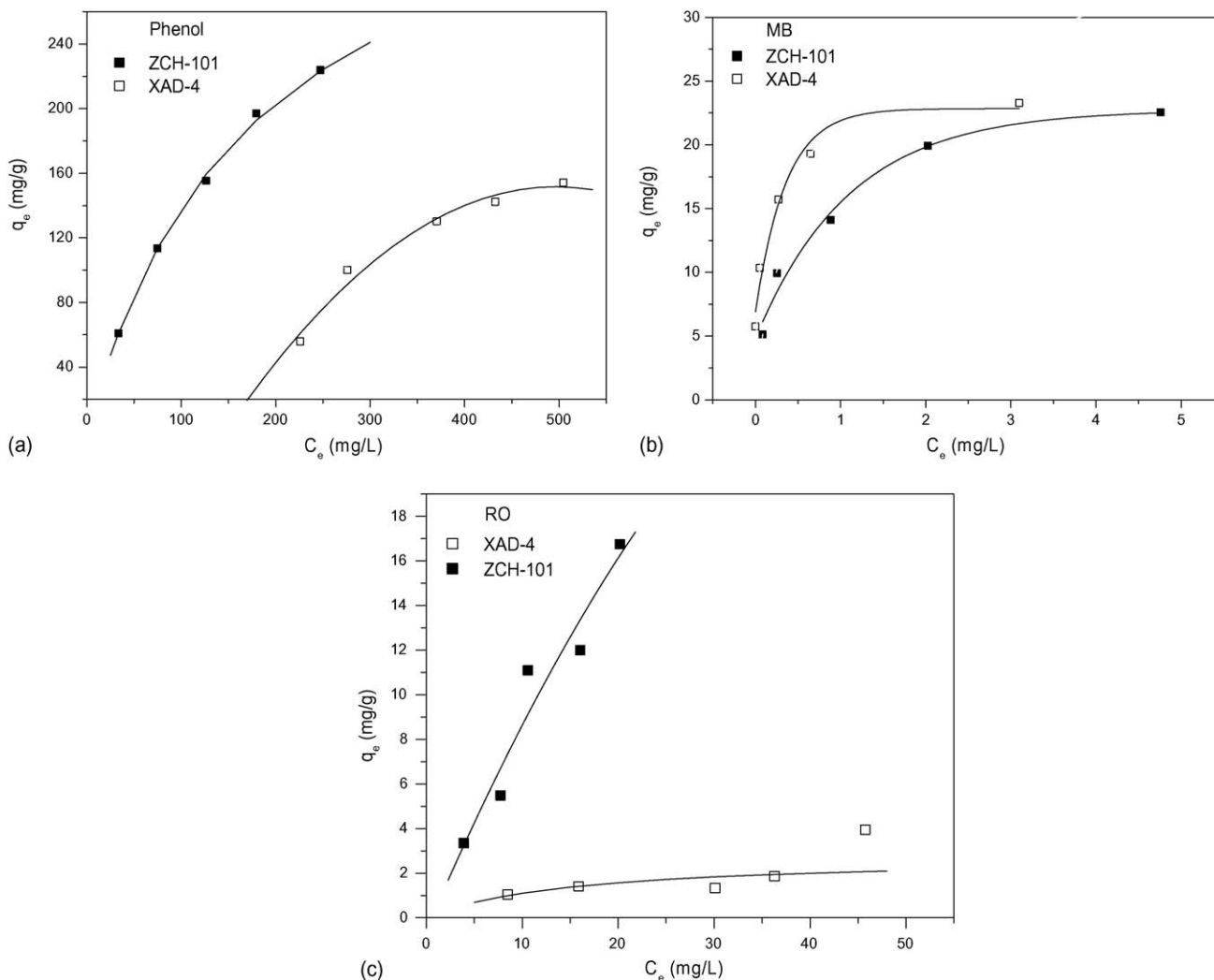


Fig. 3. Adsorption isotherms of two dyes and phenol on two resin adsorbents.

in diameter) is useless in adsorption and only a wider pore region (several times of adsorbate diameter in pore width) will be available for effective adsorption. From Fig. 2 the wider distribution of mesopore of XAD-4 is supposed to take a significant role in different capacity of MB on both adsorbents. However, ZCH-101 is more favorable in RO adsorption for its wider macropore region. In contrast, a very small macroporous region of XAD-4 causes a negligible RO adsorption on it.

The adsorption data were analyzed by the well-known Langmuir and Freundlich models [21].

### 3.2.1. Langmuir isotherm

This model assumes uniform energies of adsorption onto the surface with no transmigration of adsorbate in the plane of the surface. The linear form of Langmuir isotherm is given by the following equation:

$$\frac{1}{q_e} = \frac{1}{q_m} + \frac{1}{bq_m C_e} \quad (2)$$

where  $q_e$  is the amount adsorbed at equilibrium (mg/g),  $C_e$  is the equilibrium concentration of the adsorbate (mg/l), and  $q_m$  and

$b$  are the Langmuir constants related to maximum adsorption capacity and energy of adsorption, respectively. When  $1/q_e$  was plotted against  $1/C_e$ , a straight line obtained with slope  $1/bq_m$  indicated that the adsorption followed a Langmuir isotherm.

### 3.2.2. Freundlich isotherm

The adsorption data was also analyzed by the Freundlich model. The logarithmic form of the Freundlich model is given by the following equation:

$$\log q_e = \log K_f + \frac{1}{n} \log C_e \quad (3)$$

where  $K_f$  and  $n$  are Freundlich constants related to the adsorption capacity and adsorption intensity, respectively. When  $\log q_e$  was plotted against  $\log C_e$ , a straight line obtained with slope  $1/n$  showed that the adsorption followed a Freundlich isotherm.

Linear regression results based on the above-mentioned models were listed in Table 3. For phenol adsorption on ZCH-101 and XAD-4, both models can represent the isotherm data reasonably. Nevertheless, RO adsorption on both adsorbents does not follow any of the models. When MB adsorption is concerned,

Table 3  
Isotherm parameters for phenol and two dyes adsorption on resin adsorbents

Adsorbate	Amberlite XAD-4						ZCH-101					
	Freundlich model			Langmuir model			Freundlich model			Langmuir model		
	$K_f$	$n$	$R^2$	$q_m$	$b$	$R^2$	$K_f$	$n$	$R^2$	$q_m$	$b$	$R^2$
Phenol	1.75	1.38	0.982	476.2	0.00097	0.989	6.27	1.52	0.992	384.6	0.0056	0.999
MB	21.6	4.05	0.999	21.0	18.3	0.955	14.98	3.42	0.978	20.9	3.80	0.991
RO	0.266	1.67	0.622	2.74	0.067	0.648	0.862	1.02	0.947	232.6	0.00368	0.965

Langmuir model will be more suitable for ZCH-101 while Freundlich model will give a more satisfactory result of XAD-4.

### 3.3. Kinetics

#### 3.3.1. Concentration–time profile

The concentration–time profiles of three adsorbates on both resin adsorbents are depicted in Fig. 4(a–c). A pseudo-second-order model was proposed to evaluate the kinetic processes as

given below [22]:

$$\frac{t}{q_t} = \frac{1}{k_2 q_e^2} + \frac{t}{q_e} \tag{4}$$

where  $q_t$  is the amount adsorbed at time  $t$ ,  $k_2$  is the second rate constant. When  $t/q_t$  is plotted versus time, straight lines obtained indicating the second order adsorption kinetics.

It's clearly seen from Fig. 4 that the rate constants for all the adsorbates increase as the decrease in adsorbate size and are

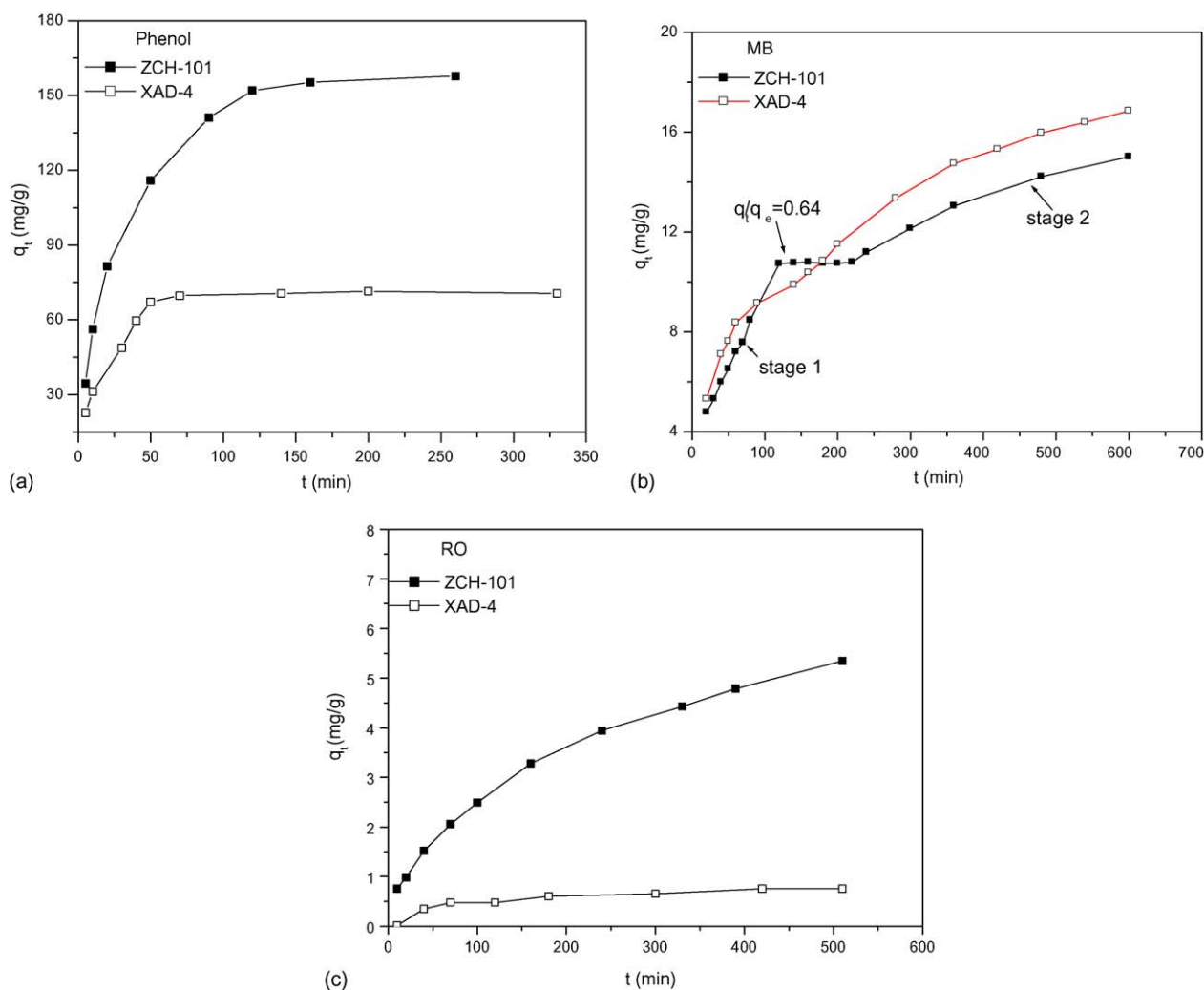


Fig. 4. Time–concentration profiles of phenol, MB and RO adsorption on both resin adsorbents.

Table 4  
Pseudo-second-order rate constants for phenol and two dyes adsorption on resin adsorbents at 298 K

Adsorbate	Amberlite XAD-4		ZCH-101	
	$k_2$ ( $\text{min}^{-1}$ )	$R^2$	$k_2$ ( $\text{min}^{-1}$ )	$R^2$
Phenol	1.2	0.993	36	0.999
MB	0.30	0.997	2.8 (stage 1)	0.991
			0.29 (stage 2)	0.999
RO	–	–	0.92	0.996

in the order phenol > MB > RO, indicating adsorbate molecules with larger size diffuse more slowly in the pore region of resin adsorbents (Table 4). A two-stage kinetic curve of MB adsorption on ZCH-101 was noteworthy and discussed in the following section.

### 3.3.2. Rate-controlling step

In general, adsorption rate of organic pollutant from aqueous solution to resin adsorbent was controlled by particle diffusion [23,24]. To validate if it is fit for adsorption in the current study,

Table 5  
Values of  $k_p$  for phenol, MB and RO adsorption on both adsorbents at 298 K ( $\text{mg/g min}^{1/2}$ )

Adsorbate	Amberlite XAD-4	ZCH-101
Phenol	16.2	9.02
MB		
$q_t/q_e < 0.64$	0.946	0.946
$q_t/q_e > 0.64$	0.456	0.784
RO	0.248	0.041

the following equation was employed as given below:

$$q_t = k_p t^{1/2} \quad (5)$$

If yes, plotting  $q_t$  versus  $t^{1/2}$  will give a straight line with a slope of  $k_p$ , where  $k_p$  is the particle diffusion coefficient ( $\text{mg/g min}^{1/2}$ ). The satisfactory validating results for three adsorbates on both adsorbents were obtained for all the relative coefficients larger than 0.99 (figures not shown). The values of  $k_p$  for phenol, MB and RO adsorption on both adsorbents (listed in Table 5) corresponds to the reverse order of adsorbate size. As

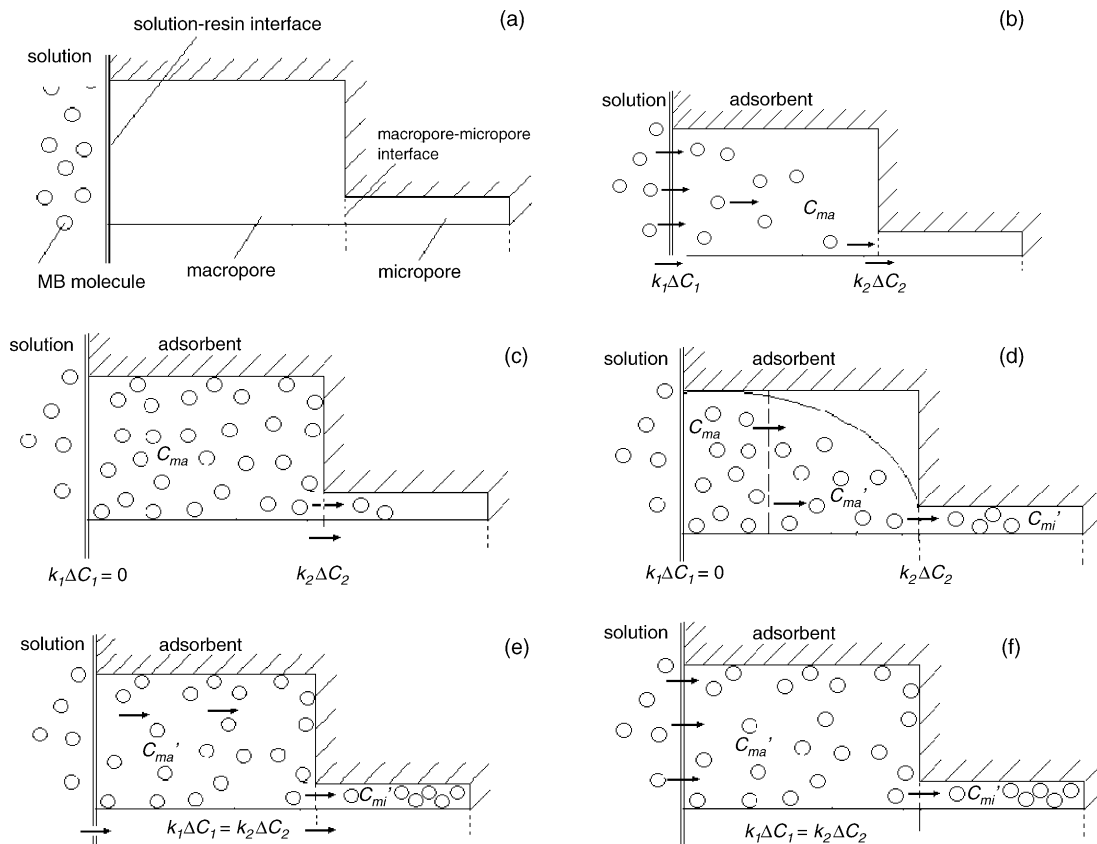


Fig. 5. Schematic illustration of MB diffusion onto resin adsorbent ZCH-101. (a) Step 1: the resin particles are put into solution but no MB molecular diffusion occurs. (b) Step 2: MB molecules diffuse from solution phase into the macropore region through the solution-resin interface at the rate of  $k_1 \Delta C_1$ . Meanwhile, diffusion occurs from macropore to micropore through an imaginary interface with a rate of  $k_2 \Delta C_2$ . (c) Step 3: MB molecules occupy all the macropore region due to the much larger value of  $k_1 \Delta C_1$  than  $k_2 \Delta C_2$  and then  $k_1 \Delta C_1$  approaches to zero, which results in the beginning of a platform in kinetic curves (as illustrated in Fig. 4(b)). Note that MB diffusion from macropore to micropore still keeps on. (d) Step 4: with the MB diffusion from macropore to micropore, the MB concentration in macropore decreases gradually and the platform in kinetic curves stands on. (e) Step 5: as MB concentration in macropore decreases, the concentration gradient between solution phase and macropore region occurs again and a new diffusion process occurs through solution-resin interface. Consequently, the platform disappears. In this step it can be concluded that the value of  $k_1 \Delta C_1$  is equal to  $k_2 \Delta C_2$ . (f) Step 6: MB diffuses until the adsorption reaches equilibrium.



for MB adsorption on ZCH-101 and XAD-4, the values of  $k_p$  at  $q_t/q_e$  less than 0.64 (for ZCH-101 it indicates the end of stage 1, as seen in Fig. 4(b)) are identical while those at  $q_t/q_e$  larger than 0.64 are different. Larger value of  $k_p$  for XAD-4 than ZCH-101 indicates more favorable adsorption of MB on XAD-4, which is consistent with the isotherm results mentioned above. Similar result can also be obtained for RO adsorption on ZCH-101, which may result from its bimodal pore distribution and especially its wider macropore region.

### 3.3.3. Schematic model of two-stage kinetic curves of MB on ZCH-101

As described above, the two-stage kinetic curve of MB adsorption on ZCH-101 should be elucidated more clearly. In order to model the MB diffusion in pore regions of ZCH-101, we assume that an imaginary interface exists between the macropore and micropore region (note that such interface does not exist really) and MB molecules diffuse into the macropore region firstly and then the micropore region. It is supposed that MB molecules diffuse from solution phase to macropore region swimmingly for the macropore width several orders of MB size. Comparatively, in micropore region MB molecules diffuse slowly for the similar size of pore width and adsorbate size. Note that surface adsorption during diffusion is not taken into account to model the kinetic process simply. Based on such assumptions a schematic model was proposed in detail in Fig. 5.

As for MB adsorption on ZCH-101, micropore diffusion can be considered as a rate-controlling step during the whole pore diffusion process. It's the diffusion rate in micropore region far less than in macropore region that results in a two-stage kinetic character, as illustrated in Fig. 4(b). Oh et al. [17] once studied phenolic derivatives adsorption on a bimodal resin adsorbent and the similar kinetic curves can also be observed in their experimental results, but such interesting observations did not gain enough attention. Note that the micropore of ZCH-101 is wide enough for phenol adsorption and useless for RO adsorption, and their kinetic curves on ZCH-101 are smooth.

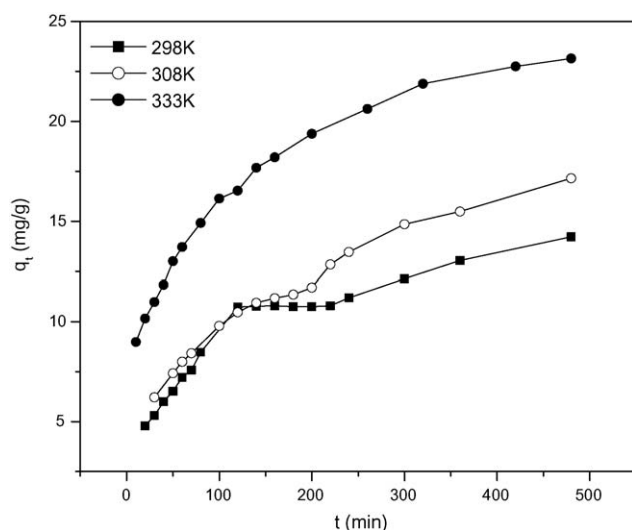


Fig. 6. Time–concentration profiles of MB adsorption on ZCH-101 at different temperatures.

In order to further validate the schematic model, additional kinetic experiments for MB adsorption on ZCH-101 were carried out at different ambient temperature and the corresponding time–concentration profiles were illustrated in Fig. 6. It can be observed that the kinetic platform interval is shortened as the ambient temperature increases and even disappears at 333 K. It may be caused by the increase in diffusion rate in micropores at a higher temperature (the value of  $k_2$  at stage 2 is  $0.29 \text{ min}^{-1}$  in 298 K and  $0.52 \text{ min}^{-1}$  at 333 K), which therefore weaken the function of micropore diffusion as a rate-controlling step. Further detailed study will be performed in future to elucidate the interesting observation.

## 4. Conclusion

In the present study adsorption of phenol and two dyes on resin adsorbents with different pore structure was discussed. The hyper-cross-linked adsorbent ZCH-101 with a bimodal pore size distribution was found more favorable than Amberlite XAD-4, a macroporous resin adsorbent, for adsorption of phenol and reactive orange X-GN. By contrast, XAD-4 was more suitable for methylene blue adsorption. A pseudo-second-order model was proved to fit all the kinetic data reasonably and the rate constant were related to adsorbate size and pore structure. Two-stage kinetics of methylene blue (MB) on ZCH-101 were observed at a specific experimental condition and modeled schematically. Such interesting kinetic curve may arise from different rate constants at macropore and micropore region and is verified by kinetic results at different ambient temperature.

## Acknowledgment

The current study was financially supported by Jiangsu Foundation of Natural Science, China (Grant no. BK2004088).

## References

- [1] J. Yoon, S. Kim, J. Byun, et al., Adsorption characteristics of direct blue 78 onto polyethylene glycol grafted polystyrene resin, *Separ. Sci. Technol.* 37 (2002) 2405–2419.
- [2] Y. Yu, Y.Y. Zhang, Z.H. Wang, et al., Adsorption of water-soluble dyes onto modified resin, *Chemosphere* 54 (2004) 425–430.
- [3] C. Long, Z.Y. Lu, A.M. Li, et al., Adsorption of reactive dyes onto polymeric adsorbents: effect of pore structure and surface chemistry group of adsorbent on adsorptive properties, *Separ. Purif. Technol.* 44 (2005) 91–96.
- [4] S. Chakraborty, S. De, S. DasGupta, et al., Adsorption study for the removal of a basic dye: experimental and modeling, *Chemosphere* 58 (2005) 1079–1086.
- [5] A. Dabrowski, P. Podkoscielny, Z. Hubicki, et al., Adsorption of phenolic compounds by activated carbon—a critical review, *Chemosphere* 58 (2005) 1049–1070.
- [6] B.C. Pan, Y. Xiong, Q. Su, et al., Role of amination of a polymeric adsorbent on phenol adsorption from aqueous solution, *Chemosphere* 51 (2003) 953–962.
- [7] W.T. Tsai, C.W. Lai, K.J. Hsien, Adsorption kinetics of herbicide paraquat from aqueous solution onto activated bleaching earth, *Chemosphere* 55 (2004) 829–837.
- [8] A.M. Li, Q.X. Zhang, H.S. Wu, et al., A new amine-modified hyper-cross-linked polymeric adsorbent for removing phenolic compounds from aqueous solutions, *Adsorpt. Sci. Technol.* 22 (2004) 807–819.

- [9] X. Zhang, Q.X. Zhang, J.L. Chen, Application of resin adsorbents in *o*-phthalic acid wastewater treatment, *Petrochem. Eng.* 29 (2000) 822–825 (in Chinese).
- [10] W.M. Zhang, L. Lv, B.C. Pan, et al., Application of resin adsorbent in wastewater treatment from synthesis of 2,6-dihydroxybenzoic acid, *Water Treat. Technol.* 28 (2002) 155–158 (in Chinese).
- [11] IUPAC, K.S.W. Sing, et al., Reporting physisorption data for gas/solid systems with special reference to the determination of surface area and porosity, *Pure Appl. Chem.* 57 (1985) 603–619.
- [12] M.M. Dubinin, H.F. Stoeckli, Homogeneous and heterogeneous micropore structure in carbonaceous adsorption, *J. Colloid Interf. Sci.* 75 (1980) 34–42.
- [13] K.S.W. Sing, The practical importance of porosity, *Chem. Ind.* 17 (1982) 475–480.
- [14] C. Petekani, The role of pore size distribution in competitive adsorption on activated carbon. Doctoral dissertation, UIUC, 1999.
- [15] Q. Li, V.L. Snoeyink, C. Campos, Displacement effect of NOM on atrazine adsorption by PACs with different pore size distributions, *Environ. Sci. Technol.* 36 (2002) 1510–1515.
- [16] B.C. Pan, Y. Xiong, A.M. Li, J.L. Chen, Q.X. Zhang, X.Y. Jin, Adsorption of aromatic acids on an aminated hyper-cross-linked macroporous polymer, *React. Funct. Polym.* 53 (2002) 63–72.
- [17] C.G. Oh, J.H. An, S.K. Ihm, Adsorptive removal of phenolic compounds by using hyper-cross-linked polystyrenic beads with bimodal pore size distribution, *React. Funct. Polym.* 57 (2003) 103–111.
- [18] M.P. Tayurupa, L.A. Andreeva, T.A. Mrachkovskaya, V.A. Davankov, Sorption of organic compounds from aqueous media by hyper-cross-linked polystyrene sorbents Styrosorb, *React. Polym.* 25 (1995) 69–78.
- [19] M.P. Tayurupa, V.A. Davankov, Hyper-cross-linked polymers: basic principle of preparing the new class of polymeric materials, *React. Funct. Polym.* 53 (2002) 193–202.
- [20] S.J. Gregg, K.S.W. Sing, Adsorption, Surface and Porosity, Chem. Eng. Press, Beijing, 1989, pp. 166–175 (in Chinese).
- [21] F.Q. Liu, J.L. Chen, A.M. Li, et al., Adsorption properties and thermodynamics of benzoic acid onto XAD-4 and a water-compatible hyper-cross-linked adsorbent, *J. Polym. Sci.* 21 (2003) 311–318.
- [22] V.K. Gupta, I. Ali, V.K. Saini, Removal of chlorophenols from wastewater using red mud: An aluminum industry waste, *Environ. Sci. Technol.* 38 (2004) 4012–4018.
- [23] W.J. Weber Jr., J.C. Morris, Kinetics of adsorption on carbon from solution, *J. Sanit. Eng. Div. Am. Soc. Civil Eng.* 89 (1963) 31–60.
- [24] Y. Yu, Dynamic adsorption process on three kinds of polystyrene adsorption resins. Doctoral dissertation, Nankai University, 2000.